

IMPROVING THE EXPERIMENTAL
CHARACTERIZATION OF ANTI-INFLUENZA DRUG
EFFICACY USING MATHEMATICAL MODELS

by

Wendy Wong

April 13, 2010

A thesis

presented to the Department of Physics

in partial fulfillment of the

requirements for the degree of

Bachelor of Science

in the Program of

Medical Physics

at Ryerson University

Supervisor: Dr. Catherine Beauchemin

Abstract

With the emergence of drug-resistant viral strains, effective characterization of an antiviral drug's efficacy against a specific viral strain is important. A commonly used method in characterizing the effectiveness of an antiviral drug against a particular strain of virus is by measuring the IC_{50} . The IC_{50} is defined as the concentration of drug necessary to inhibit half of a particular viral effect in vitro. However, there are problems associated with using existing methods in estimating the IC_{50} . One problem involves the time at which experimentalists decide to take measurements in calculating the estimate of the IC_{50} . Because of this, the estimate of the IC_{50} for any given drug-strain pair could vary widely between laboratories. Also, there are discrepancies between the experimentalist's definition of the IC_{50} , and the mathematical modeller's definition of the IC_{50} . Most experimentalists would consider the IC_{50} as the drug concentration required to halve the population of what you are measuring e.g. virus [5] or dead cells [13]; the IC_{50} then would only be relevant at the macroscopic level. The modeller's definition of the IC_{50} assumes that the drug affects the interaction between the virus and the cell, and that the IC_{50} is the drug concentration needed to halve some effect at the microscopic level e.g. the rate at which virus is produced by an infected cell. It would be advantageous to have an experiment where the estimate of the IC_{50} can be reliably calculated so that laboratory measurements would yield more consistent results, and where there is minimal difference between the experimentalist's IC_{50} and the modeller's IC_{50} for a specific drug-strain pair. In this thesis, both problems are considered using a theoretical and mathematical technique.

Acknowledgements

I want to express my gratitude to a number of individuals who have motivated me, and who have kindly offered me assistance through the course of my research.

Firstly, this work would not have been possible without the guidance of my supervisor Dr. Catherine Beauchemin.

Secondly, I would like to thank Dr. Benjamin Holder for the help he has provided me. Many of the problems I have encountered during this thesis would not have been solved quite as easily without his patience and expertise.

Moreover, I am grateful for the valuable knowledge I have gained through the meetings I have attended with the Phymbie group.

Lastly, I would like to extend a warm thank you to all the individuals who have had a positive influence in my undergraduate career (there's too many to name), with special thanks to Azfar, Karen, Shanthi, and Sheena.

Table of Contents

Abstract	ii
Acknowledgements	iii
Table of Content	iv
List of Tables	vi
List of Figures	vii
1 Introduction	1
2 Materials and Methods	6
2.1 The mathematical model	6
2.2 Single cycle growth	9
3 Results and Discussion	12
3.1 Estimating the IC_{50} from virus produced in viral yield experiments	12
3.2 Estimating the IC_{50} from infection-induced cell death in viral yield experiments	15
3.3 Proposal for using single cycle growth to estimate IC_{50}	21

4 Conclusion	25
Bibliography	27
A Solution to the single cycle growth calculations	31

List of Tables

2.1	Value of the model's parameters	8
-----	---	---

List of Figures

3.1	Characterizing the effect of antiviral treatment from viral titer measurements	16
3.2	Dependence of IC_{50} estimates extracted from viral titers on the measurement time	17
3.3	Characterizing the effect of antiviral treatment from the progression of cell death.	19
3.4	Dependence of IC_{50} estimates extracted from the progression of cell death on the measurement time.	20
3.5	Dependence of IC_{50} estimates extracted from viral titer measurements in single cycle growth experiments	23
3.6	The effect of experimental variability on IC_{50} estimates from single cycle growth experiments	24

Chapter 1

Introduction

In recent years, influenza has received a lot of media attention, featuring avian influenza (H5N1) and its potential to be transmitted from avian species to mammalian species including humans [8], the emergence of swine-origin H1N1 last year, and the growing trend of influenza strains becoming resistant to existing antiviral drugs [9]. On June 11, 2009 only two months after the first human infections with a novel influenza A (H1N1) virus of swine origin were reported by Mexico and the United States, the World Health Organization declared the first influenza pandemic of the 21st century [9]. Since vaccines can not be prepared quickly enough in the event of a pandemic, due to the lengthy processes involved in testing and manufacturing [7], other measures of control are needed to contain a pandemic at its earliest phases. In a pandemic, antiviral drugs are our first line of defense against new influenza strains both in prevention and in treatment [2]. They can be highly effective in prophylaxis, and shorten the duration of illness by up to 1.5 days when used in treatment [4, 11]. Since there is a heavy reliance on antiviral drugs to counter infections during the initial stages of a pandemic, characterization

of a virus strain's resistance to a particular antiviral drug is important.

Currently, there are two classes of antiviral drugs available for use against influenza: adamantanes e.g. amantadine and rimantadine, and neuraminidase inhibitors e.g. oseltamivir and zanamivir. The former are limited in activity to influenza A viruses, whereas the latter are active against influenza B viruses as well [6]. Adamantanes are commonly known as M2 inhibitors because they act by inhibiting the action of the M2 protein channels. The M2 channel of the influenza A virus is a pH-activated proton channel that mediates acidification of the interior of viral particles entrapped in endosomes [18]. Thus, an M2 blocker will prevent the virus capsule from opening and start replication after cell entry. The use of adamantanes can cause the influenza virus to acquire a mutation which will cause the M2 protein to become resistant to these drugs without losing its regular activity [3]. The mutated virus will be resistant to these drugs, and even in the presence of adamantanes the virus will be able to release the viral proteins for replication. In the United States, the frequency of the adamantane-resistant influenza during the regular influenza season at the beginning of 2004 was 1.9%, between 2004 and 2005 it escalated to 14.5%, and at the beginning of 2006 it reached frequency of 92% [19].

Neuraminidase inhibitor drugs oseltamivir (Tamiflu) and zanamivir (Relenza) work by inhibiting one of the key surface proteins of the influenza virus, the neuraminidase, which in turn decreases the ability of the virus to infect other cells in the respiratory tract [3]. The neuraminidase plays a vital role during the final stages of virion budding from infected cells; if the neuraminidase enzyme is inhibited, newly produced virions are not released from the surface of the cell which produced them [3]. The neuraminidase viral enzyme cleaves the terminal

sialic acid from the cellular receptor, to which newly formed virions are attached. This cleavage releases the progeny virions from the infected cell, enabling them to infect other cells [3]. By blocking this releasing mechanism, the virus completes replication only once, preventing further infection [16]. Our reliance on these two drugs has intensified because of extremely high levels of resistance with influenza viruses to the other class of antiviral drugs, the adamantanes [3, 6]. Oseltamivir and zanamivir are the most widely-used drugs and are effective against influenza A and influenza B infections [12].

After the introduction of widely-used antiviral drugs, drug-resistant virus strains began to emerge [12, 17, 19]. Because influenza viruses can mutate at high frequencies and evolve rapidly, the genotypes encoding drug resistance can arise rapidly [3]. Drug resistant genotypes may be at an advantage in hosts where the drug is present and may become the dominant genotypes under these conditions [17]. Therefore, in treated infections, the drug will be less effective against drug-resistant strains of virus versus virus that do not have the mutation conferring resistance to the drug. The measure of drug resistance of a particular virus is a relative value rather than an absolute value; this means that the drug-resistance of a particular strain of influenza is only useful in comparison with that of another strain of influenza.

A measure of the degree of resistance can be obtained by determining an estimate of the 50% inhibitory concentration (IC_{50}) of a specific antiviral drug against a given viral strain. The IC_{50} is the drug concentration needed to inhibit half of a particular effect [14]. For example, if the same drug is used on both virus A and virus B, and the estimate of IC_{50} for virus A is 0.3 nM, whereas the estimate of IC_{50} for virus B is 0.1 nM, one can say that virus B is more sensitive to the drug

than virus A because less of the same drug (one-third less in this example) can be applied to virus B to obtain the same biological effect as with virus A. This also means that virus A is mildly resistant to the antiviral drug compared to virus B because more of the drug would be required to yield the same effect.

There are two main methods for characterizing the estimate of the IC_{50} of an antiviral drug against a specific viral strain. In the biology community, most experimentalists would identify the estimate of the IC_{50} as the concentration of drug that would halve the population of what you are measuring e.g. virus, fraction of dead cells. In this sense, the estimate of the IC_{50} would only be relevant on a macroscopic scale.

Mathematical models are useful in helping researchers analyze experimental results and comprehend the meaning behind the results of experiment. Constructing mathematical models of experimental procedures allows us to better understand what experiments are truly measuring and how their results may vary for the same drug-strain pair. As a result, mathematical models are a useful tool in supplementing experiments, and can assist researchers in implementing changes to their experimental methods and procedures, and to improve their relevance and accuracy. In a mathematical model, the IC_{50} is defined at the level of the virus-cell interaction, for example, the amount of drug required to halve the virus production of a cell. This definition of the IC_{50} assumes that a drug acts at the microscopic level of interaction between virus and cell, and that the IC_{50} is a measure of the drug concentration necessary to halve some effect at that level.

Because the estimate of the IC_{50} is a common method used to compare the resistance of different strains of virus, and consequently the effectiveness of antiviral drugs against resistant and sensitive strains of virus, the techniques used to extract

the estimate of the IC_{50} should be reliable. However, there is speculation that in many cases the estimate of the IC_{50} found from different experimental techniques are erroneous due to various factors; one example would be the measurement time. This is significant because this would imply that some previous conclusions drawn from the estimate of the IC_{50} on the resistance of assorted strains of virus could be incorrect.

The purpose of this thesis is to determine to which extent experimentally-derived estimates of the IC_{50} fluctuate as a result of different experimental factors, such as measurement time. Also, it would be of interest to propose an experimental method where the discrepancies between the experimentalists' and the modellers' definition of the IC_{50} would be minimal.

Chapter 2

Materials and Methods

2.1 The mathematical model

A set of ordinary differential equations were used to simulate the dynamics of experimental influenza infections in vitro. The delay model utilized consists of the number of cells in the target, latently-infected phase, productively-infected phase, and the viral titer [1]. Cells in the target phase are uninfected, and would eventually become infected and move into the latently-infected phase of infection. Cells in the latently-infected phase are awaiting the moment in which they become cells that produce virus. Cells in the productively-infected phase are actively producing virus. This model can be mathematically represented in the following

way,

$$\frac{dT}{dt} = -\beta TV \quad (2.1)$$

$$\frac{dL}{dt} = \beta TV - \frac{L}{\tau_L} \quad (2.2)$$

$$\frac{dI}{dt} = \frac{L}{\tau_L} - \frac{I}{\tau_I} \quad (2.3)$$

$$\frac{dV}{dt} = (1 - \varepsilon)pI - cV \quad (2.4)$$

where β is the rate at which target cells, T , are infected by the virus, V , and enter the latently-infected state, L . After an average time τ_L , the latently-infected cells, L , become productively-infected, I . Productively-infected cells, I , produce virus, V , continuously at rate p , and eventually die from viral cytotoxic effects after producing virus for an average time τ_I . Finally, virus is cleared at a rate, c , as it gradually loses infectivity. Neuraminidase inhibitors affect the rate at which virus is released from cells in the productively-infected phase. In our model, there is no distinction between virus production and virus release; therefore neuraminidase inhibitors are modelled as acting on the viral production rate, p , with an efficacy $0 \leq \varepsilon < 1$. The relationship between drug efficacy, ε , and drug concentration, D , is captured using the ε_{\max} model, namely

$$\varepsilon = \frac{\varepsilon_{\max} D}{D + IC_{50}} \quad (2.5)$$

where D is the drug concentration, ε_{\max} is the maximum or the saturation efficacy of the drug, and IC_{50} is the drug concentration at which drug efficacy is half its maximum value. Over the course of experiments, the drug concentration is considered to be more or less constant. So in our simulations, D is fixed over time

Name	Value
β	$3.2 \times 10^{-5} \text{ (TCID}_{50}/\text{mL})^{-1} \cdot \text{d}^{-1}$
τ_L	6 h
τ_I	4.56 h
p	$4.0 \times 10^{-2} \text{ (TCID}_{50}/\text{mL}) \cdot \text{d}^{-1}$
$\frac{1}{c}$	4.56 h
IC_{50}	2.8 nM
ε_{\max}	1.0

Table 2.1: Value of the model’s parameters. The influenza kinetic parameters (above the line) were taken from Table 3 of Baccam et al. [1]. Parameters relating to the drug’s efficacy (below the line) were chosen to represent a realistic example for treatment with zanamivir [5].

for a given simulation. When drug is added through ε , a theoretical estimate of the IC_{50} of 2.8 nM is used. This value was obtained from the experiments performed by Eichelberger et al. [5], and will serve as a reference value for all simulations for the treatment of an in vitro infection with A/Memphis/14/98 (subtype) with zanamivir.

Two common experiments for the measure of the IC_{50} estimates were simulated, both of which were initiated under the same circumstances: infections start as a result of an inoculation of infectious virus, and the initial conditions are $T_0 = 4 \times 10^8$ cells, $L_0 = 0$, $I_0 = 0$, $V_0 = 7.5 \times 10^{-2} \text{ TCID}_{50}/\text{mL}$. For all of the parameters and initial conditions, we used values for the delay model presented in Table 3 of the Baccam et al. paper [1], listed here in Table 2.1.

In the first type of experiment modelled, the amount of virus at a particular measurement time is measured. In the second type of experiment, the fraction of dead cells are sampled at a particular measurement time. The fraction of dead

cells at any particular time can be computed using the following equation:

$$\text{fraction of dead cells} = 1 - \frac{T_t + L_t + I_t}{T_0} \quad (2.6)$$

where T_t is the number of target cells at a particular measurement time, t , L_t is the number of cells undergoing the latently-infected phase at a particular measurement time, I_t is the number of cells that are productively-infected at a particular measurement time, and T_0 is the initial number of target cells present in the experiment. In each case, the IC_{50} is estimated by comparing the results, either the virus concentration or the fraction of dead cells at the time they are measured, over a wide range of applied drug concentrations, D .

The set of ordinary differential equations in the delay model are solved by using the `lsode` solver in Octave. The `lsode` function returns a matrix of values for the remaining number of target cells, the number of cells in the latently-infected phase, the number of productively-infected cells, and the viral titer for select times post-infection.

All the scripts used in this project were developed by me with some assistance from Dr. Catherine Beauchemin and Dr. Ben Holder.

2.2 Single cycle growth

A new method for estimating the IC_{50} from in vitro experiments is proposed, using single cycle viral growth. The single cycle growth method is able to give an accurate estimate of the drug's efficacy on ρ but not on the other parameters. Because of this limitation, the single cycle growth experiment is not suitable for

estimating the IC_{50} of an M2 inhibitor. Single cycle growth can be simulated with the delay model [1], however adjustments have to be made to the model so that the characteristics of a single cycle growth will be shown by the model. For the simulations, the initial conditions for single cycle growth are that all the cells are in the productively-infected phase:

$$\frac{dI}{dt} = -\frac{I}{\tau_I} \quad (2.7)$$

$$\frac{dV}{dt} = \rho I - \frac{V}{\tau_V} \quad (2.8)$$

The above equations can be rearranged into a linear non-homogeneous ordinary differential equation,

$$\frac{dV}{dt} + cV = \rho N e^{-\frac{t}{\tau_I}} \quad (2.9)$$

In this equation, c is the clearance rate of viruses, V is the initial viral titer, where ρ is equal to $(1 - \varepsilon)p$ and p is the viral production rate, N is the number of productively-infected cells (which is all the cells), and τ_I is the average time of virus production of an infected cell.

There are two different scenarios of single cycle growth that could be simulated, one involves neglecting viral clearance and productively-infected cell death, and the other involves neglecting only cell death.

When viral clearance of virus, c , and productively-infected cell death, $\frac{1}{\tau_I}$ are neglected, the equation is easily integrated as

$$\frac{dV}{dt} = \rho N \Rightarrow V(t) = V_0 + \rho N t \quad (2.10)$$

When only productively-infected cell death is neglected, the equation above can be solved (see Appendix A for full solution) as:

$$V(t) = V_0 e^{-ct} + \frac{\rho N}{c} (1 - e^{-ct}) \quad (2.11)$$

Here, V_0 represents the initial number of viruses, this term can be ignored because the original viruses used to infect the cells are removed prior to the beginning of the experiment, therefore this term can be set to zero. This would then result in the following equation which will be used to simulate a single cycle growth experiment.

$$V(t) = \frac{\rho N}{c} (1 - e^{-ct}) \quad (2.12)$$

Chapter 3

Results and Discussion

In this chapter, the mathematical model (a set of ordinary differential equations) is applied to simulate two different experimental systems, one will utilize viral titer in estimating the IC_{50} , and the other will estimate the IC_{50} from cell death. In each simulation, a theoretical estimate of the IC_{50} of 2.8 nM is inserted into the ε_{\max} model, and its effect is applied to virus production. Using the mathematical model, variations between the measured estimate of the IC_{50} at different measurement times will be analyzed. Moreover, the outcome of the experimentally measured estimate of the IC_{50} is investigated to see if it corresponds to the theoretical IC_{50} input into the model.

3.1 Estimating the IC_{50} from virus produced in viral yield experiments

There are an assortment of methods used in measuring viral titer, the majority require staining of the virus. Viral specimens can be negatively stained and ex-

amined in an electron microscope for the presence of virions [3]. However, there are limitations to this approach because of the high costs of the equipment, and the limited sensitivity of stains that are currently available. Most stains that are available have a minimum detectable concentration of virions of approximately 1,000,000/mL [3]. One method for counting the number of virus present is by quantifying the neuraminidase activity that occurs when virus particles emerge from infected cells [15]. One such technique involves the use of a fluorescent substrate, methyl-umbelliferyl-N-acetyl neuraminic acid (MU-NANA) that can quantify the neuraminidase activity, as demonstrated in the experiments performed by Eichelberger et al. [5]. The neuraminidase activity is one way to measure viral titer since the activity should be proportional to the number of virions.

One method used in estimating the IC_{50} of an antiviral drug for a specific viral strain is by detecting the amount of virus in the presence of various concentrations of the drug, and in the absence of the drug. When drug concentration increases, a reduction in viral titer occurs; thus, a decrease in viral titer as a consequence of the addition of an antiviral drug is one way to characterize the efficacy of a drug. The effect of different concentrations of drug on viral titer is shown in Figure 3.1a, using the parameters from Table 2.1, and the mathematical model. In Figure 3.1a, the viral titer peaks between the second or third day post-infection in the absence of drug. As the drug concentration increases from zero to a concentration corresponding to the theoretically applied IC_{50} (2.8 nM) of the drug, the peak of the viral titer is reduced, and the growth of the virus is delayed. The dotted line in the graph represents an example of a measurement time at which the viral titer is taken.

The estimate of the IC_{50} is typically defined experimentally as the amount of

drug required so that the viral titer at the chosen measurement time, e.g. 48 h post-infection, is half that in the absence of any drug. Using the data in Figure 3.1a as an example, it is possible to plot the viral titer at 48 h as a function of drug concentration, as shown in Figure 3.1b. In this example, the viral titer measurements are taken at 48 h because it is prior to when the viral titer curves begin to peak; this is crucial because if measurements were to be taken at times after the viral titer peaks (when viruses start to undergo clearance), it could result in misleading and erroneous outcomes. From this graph, the estimate of the IC_{50} corresponds to the drug concentration at which the normalized viral concentration is halved (i.e. equal to 0.5), and the estimate of the IC_{50} is approximately 0.3 nM.

Figure 3.2a shows the results of the simulation using a continuous range of drug concentrations, for six different measurement times. Each curve represents a measurement time at which the estimate of the IC_{50} may be extracted. It is obvious that the estimates of the IC_{50} would not be the same if the samples of viral titer were to be taken at different measurement times. At later measurements, the graph shifts toward the right. This indicates a decrease in the estimate of the IC_{50} . In comparing the estimate of the IC_{50} taken at the earliest measurement time of 8 h, which was about 2 nM, to that of a later measurement time at 48 h which had an IC_{50} value of around 0.2 nM, one would observe a difference of about one order of magnitude between the two estimates of IC_{50} .

When more frequent samples of the viral titer are taken for different measurement times, a functional shape for how the estimate of the IC_{50} varies as a function of the measurement time emerges as shown in Figure 3.2b. The estimate of the IC_{50} for various measurement times from Figure 3.2b further supports that presented in Figure 3.2a, by demonstrating how the estimates of the IC_{50} decline when

the measurements of viral titer are taken at later times. This reinforces the idea that the estimate of the IC_{50} is dependent on the measurement time chosen by the experimentalist to sample the viral titer in estimating the IC_{50} .

3.2 Estimating the IC_{50} from infection-induced cell death in viral yield experiments

The cytopathic effect (cell death) induced by a viral infection, is a determinant for the proliferation of viruses [10]. One method in measuring cell death involves a cell based luminescence assay utilized for screening the amount of live cells or cell viability in the culture [13]. When the viral titer increases, there will also be an increase in cytopathic effects in the culture.

In a typical viral infection, the viral titer will increase over time as an increasing number of target cells become infected and begin to actively-produce viruses. When the viral titer rises, it is followed by an increase in the fraction of dead cells. At the initial phase, there are no dead cells present because the majority of cells in the culture will still be target cells, and the cells that have become infected with the virus would be progressing through the latently-infected, and actively producing virus phase of infection; thus, little or no cytopathic effect would be detected early on in the infection. But as the infection continues, the fraction of dead cells will gradually increase. Ultimately, all cells within the culture will die.

Figure 3.3 shows the simulated increase in the fraction of dead cells over time when a variety of drug concentrations are applied, using the mathematical model and parameters from Table 2.1. As the drug concentration increases, less virus is produced by the infected cells. Because of the reduction in the viral titer, it will

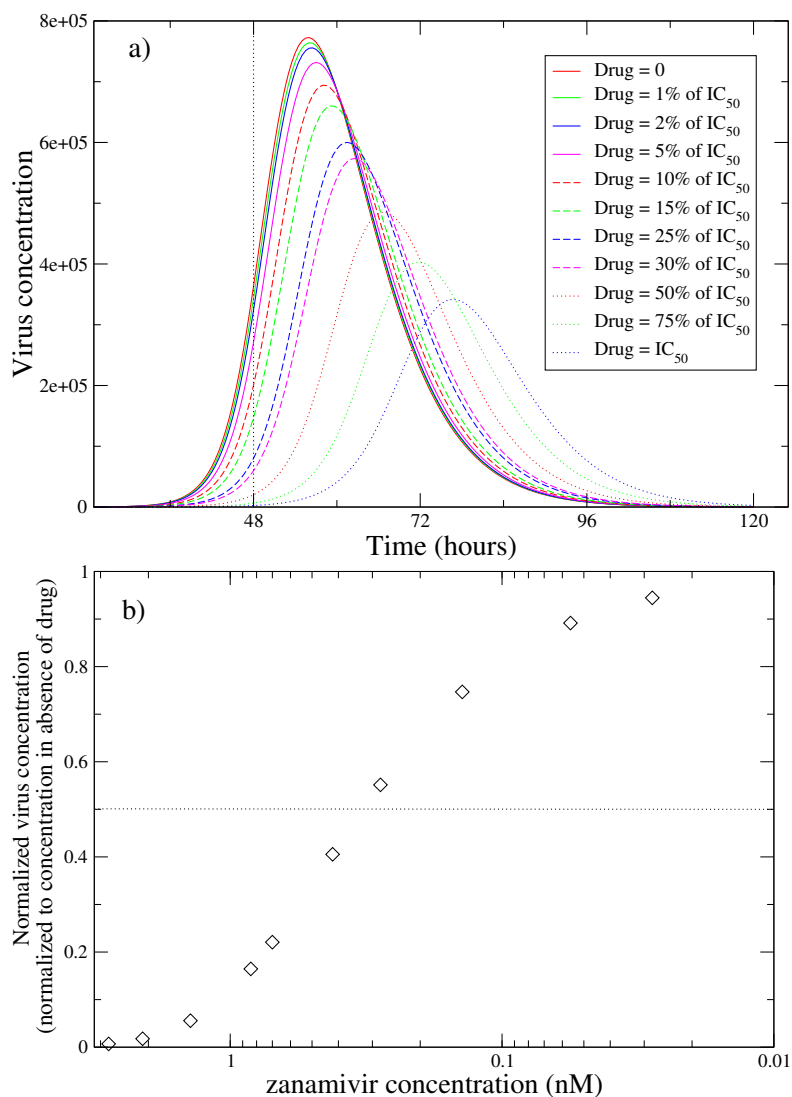


Figure 3.1: Characterizing the effect of antiviral treatment from viral titer measurements. a) The effect of different antiviral drug concentrations on virus concentration; the applied drug concentration is defined relative to the IC_{50} of the antiviral drug for that influenza strain. The vertical dotted line represents a point in time at which a measurement can be taken. b) Normalized virus concentrations for different drug concentrations at the measurement time of 48 h. The horizontal dotted line represents the point at which the normalized viral concentration is half that in the absence of antiviral drug treatment. The intersection of the dotted line and the curve is taken to correspond to the IC_{50} for this particular drug-strain pair (about 0.3 nM for the case illustrated here).

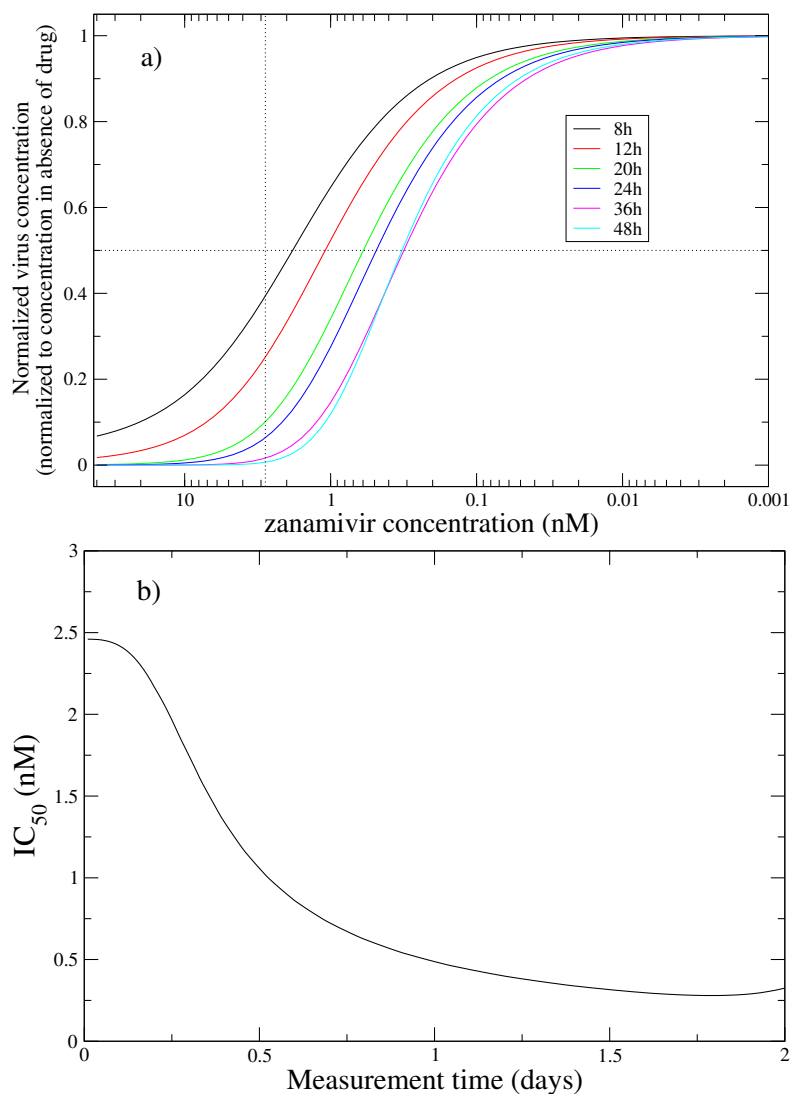


Figure 3.2: Dependence of IC_{50} estimates extracted from viral titers on the measurement time. a) The effect of drug concentration on viral titer when the latter is measured at different times. This illustrates that the IC_{50} estimates (the zanamivir concentration at which the curves cross the horizontal dotted line) depends on the measurement times. The vertical dotted line corresponds to the input value of the IC_{50} which is 2.8 nM. b) The effect of measurement time on the estimate obtained for the IC_{50} . The estimate is neither independent of the measurement time, nor does it ever match the input/correct value of 2.8 nM at any measurement time.

take longer for target cells to become infected, compared to the case where no drug is applied. The dotted line in the graph represents an example of a measurement time that might be chosen by an experimentalist to measure the fraction of dead cells in each infection experiment where different drug concentrations were used. The IC_{50} is estimated as the drug concentration at which the fraction of dead cells is half the fraction of dead cells measured in the absence of drug at that measurement time.

Figure 3.4a shows the fraction of dead cells (normalized to the fraction of dead cells with no drug applied) as a continuous function of applied drug concentration and for a variety of measurement times. It is clear that the estimate of the IC_{50} would not be the same if the samples of fraction of dead cells were to be taken at different measurement times. In Figure 3.4a, as the measurement time increases, the plots on the graph shifts toward the left, indicating an increase in the estimate of IC_{50} . So, at later measurement times, one would get a larger estimate of the IC_{50} compared to that at earlier measurement times. As well, this demonstrates the time-dependence of the estimate of the IC_{50} on the measurement time.

The graph in Figure 3.4b illustrates how the estimate of the IC_{50} changes as a function of the measurement time. Figure 3.4b demonstrates how the estimate of the IC_{50} increases, when the fraction of dead cells samples are taken at later measurement times.

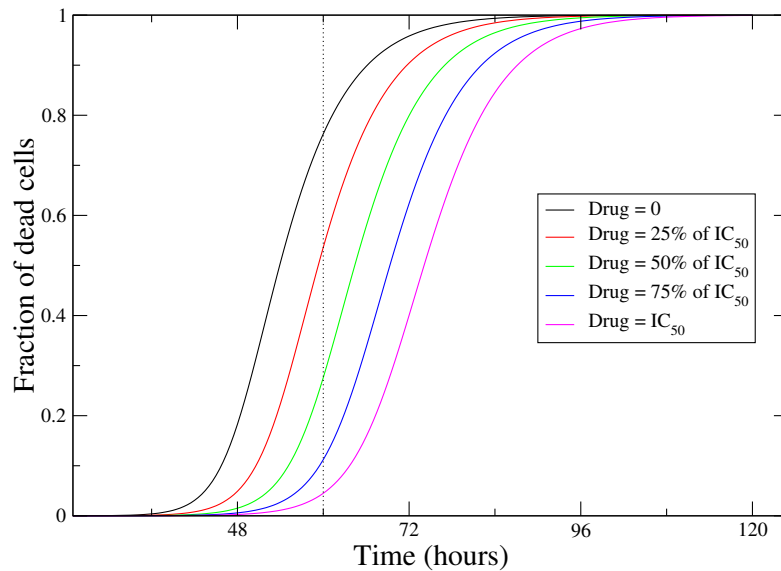


Figure 3.3: Characterizing the effect of antiviral treatment from the progression of cell death. The progression of cell death (fraction of dead cells) as a function of time is illustrated for different drug concentrations. As the applied drug concentration increases, the graph shifts towards the right indicating a delay in cell death. Note that, for example, at a measurement time of 60 h (vertical dotted line) the IC_{50} estimate which corresponds to the drug concentration required to halve the fraction of dead cells observed in the absence of treatment (half the value at which the black line crosses the dotted line, so around 0.37) corresponds to about 25%–50% of the correct/input IC_{50} (i.e. between the red and green lines).

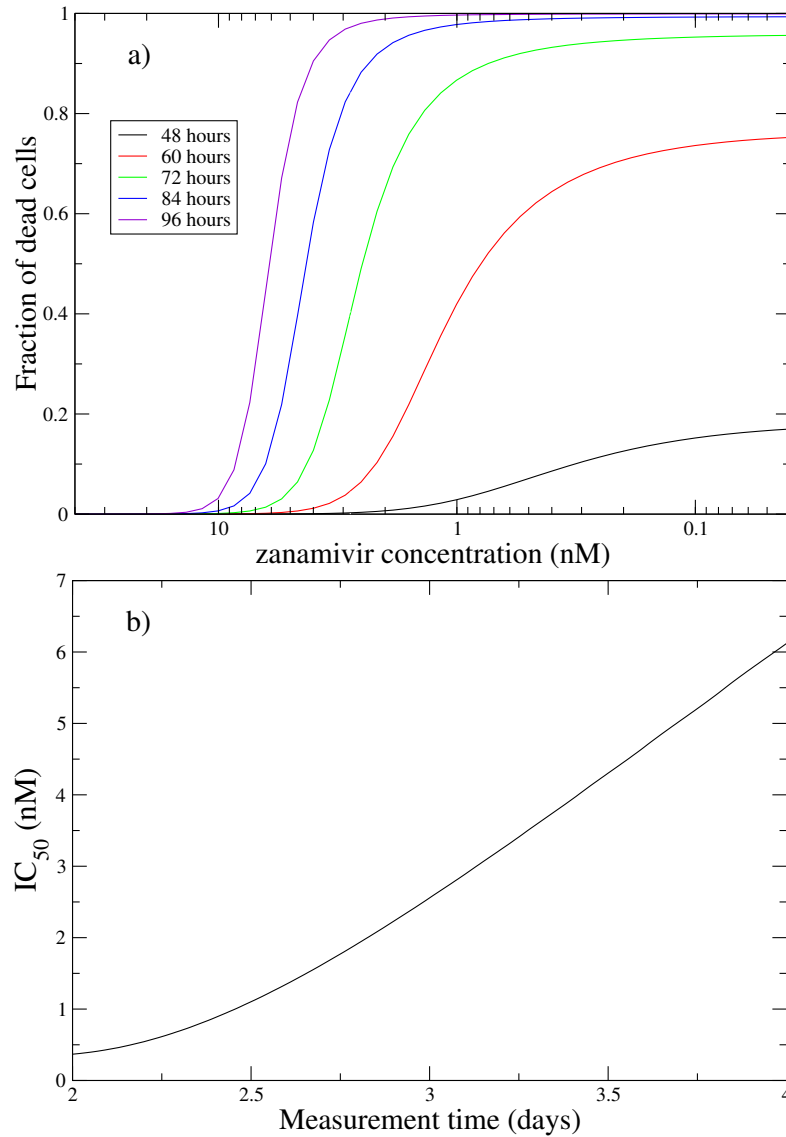


Figure 3.4: Dependence of IC_{50} estimates extracted from the progression of cell death on the measurement time. a) The effect of drug concentration on the fraction of dead cells present in the culture. b) The effect of measurement time on the estimate obtained for the IC_{50} . The IC_{50} estimate is larger for later measurement times.

3.3 Proposal for using single cycle growth to estimate IC_{50}

Single cycle growth experiments are similar to multiple cycle growths experiments presented previously in this chapter, in that cells are infected with an initial concentration of virus, and the resulting virus concentration is measured over time. In contrast to multiple cycle growth experiments, however, single cycle growth experiments begin with a much higher concentration of virus, so that it can be assumed that all cells are initially infected. In other words, single cycle growth experiments have a high multiplicity of infection (MOI), a large ratio of infectious agents e.g. viruses to target (uninfected) cells; contrary to multiple cycle growth experiments where the multiplicity of infection (MOI) are relatively low. After the entire population of target cells are infected, the original virus inoculum used to infect the cell culture is removed from the experimental system. The cells infected with the virus continue into the latently-infected phase, and afterwards, into the productively-infected phase of the infection. The virus count in the single cycle growth experiments includes only virus produced by the productively-infected cells. Instead of the exponential growth that takes place in multiple cycle growth experiments, in single cycle growth experiments virus grows linearly in time. Because of this unique property, single cycle growth experiments shows promise as a possible solution to the problems arising from existing methods used in estimating the IC_{50} of drug-strain pairs.

A range of measurement times were chosen for the single cycle growth simulation: 3 h, 6 h, 9 h, 12 h, and 15 h, and results are shown in Figure 3.5. Despite the selection of different measurement times, the normalized viral titers measured at

each individual measurement time are the same. Which is why, in Figure 3.5, the viral titer plots for different measurement times are overlapping one another, since their viral titers are the same. More importantly, the estimate of the IC_{50} observed in Figure 3.5 is equal to the theoretical estimate of the IC_{50} (2.8 nM) input in the ε_{\max} model. In Figure 3.5, the estimate of the IC_{50} is shown where the horizontal dotted line and the curve intersects. From Figure 3.5, single cycle growth experiments shows potential in being a valid option in consistently estimating the IC_{50} for neuraminidase inhibitors since it can minimize the aberrations in the estimate of the IC_{50} between various measurement times, and eliminates the disagreement between the biological estimate of the IC_{50} and the ε_{\max} model's estimate of the IC_{50} .

To investigate the robustness of the estimates of the IC_{50} computed from the single cycle growth experiments, the same type of measurements were taken but Gaussian noise was added to the simulated data. Figure 3.6 shows 4 separate measurement times (3, 6, 9, and 12 h) at which the virus concentration was measured for the single cycle growth experiment in the presence of simulated experimental variability. Figure 3.6 was generated using the data presented in Figure 3.5 in combination with error following a Gaussian distribution. A sigma of 10% was chosen for the error distribution because this was approximately the error shown in previous single cycle growth experiments. Figure 3.6 shows that even with error in the single cycle growth experiment, the estimate of the IC_{50} can be reliably obtained, and is very similar to the estimate of the IC_{50} (2.8 nM) placed in the ε_{\max} model. This further establishes that the single cycle growth experiment is a robust way of estimating the IC_{50} of a drug-strain pair when evaluating neuraminidase inhibitors.

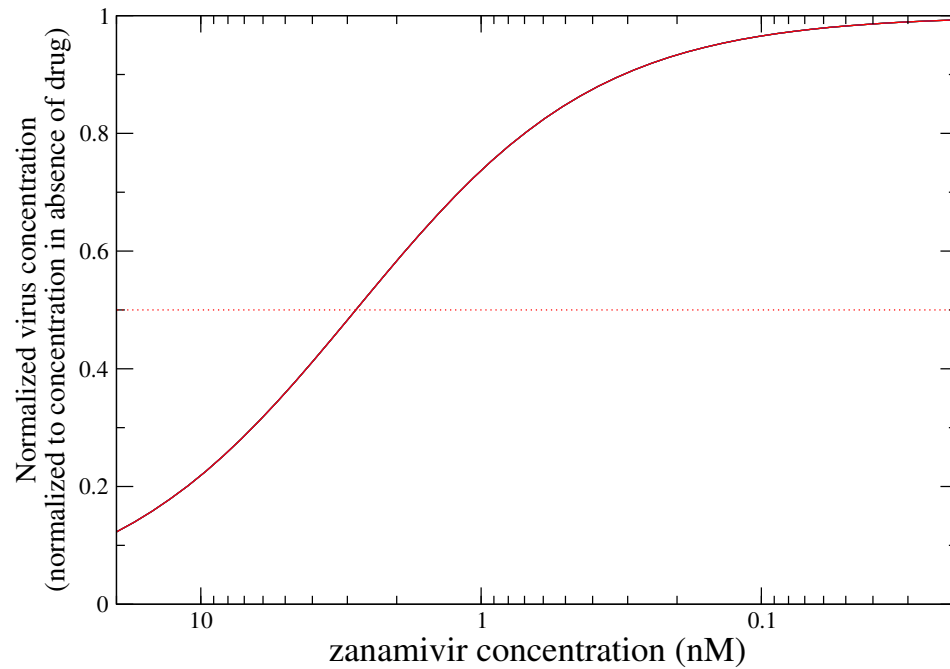


Figure 3.5: Dependence of IC_{50} estimates extracted from viral titer measurements in single cycle growth experiments. Multiple curves of normalized viral titers versus drug concentration are shown here for several measurement times but cannot be seen as they all overlap, i.e. the normalized viral titers obtained are independent of the time at which measurements are taken. As a result, the IC_{50} estimates extracted from these measurements does not depend on measurement time.

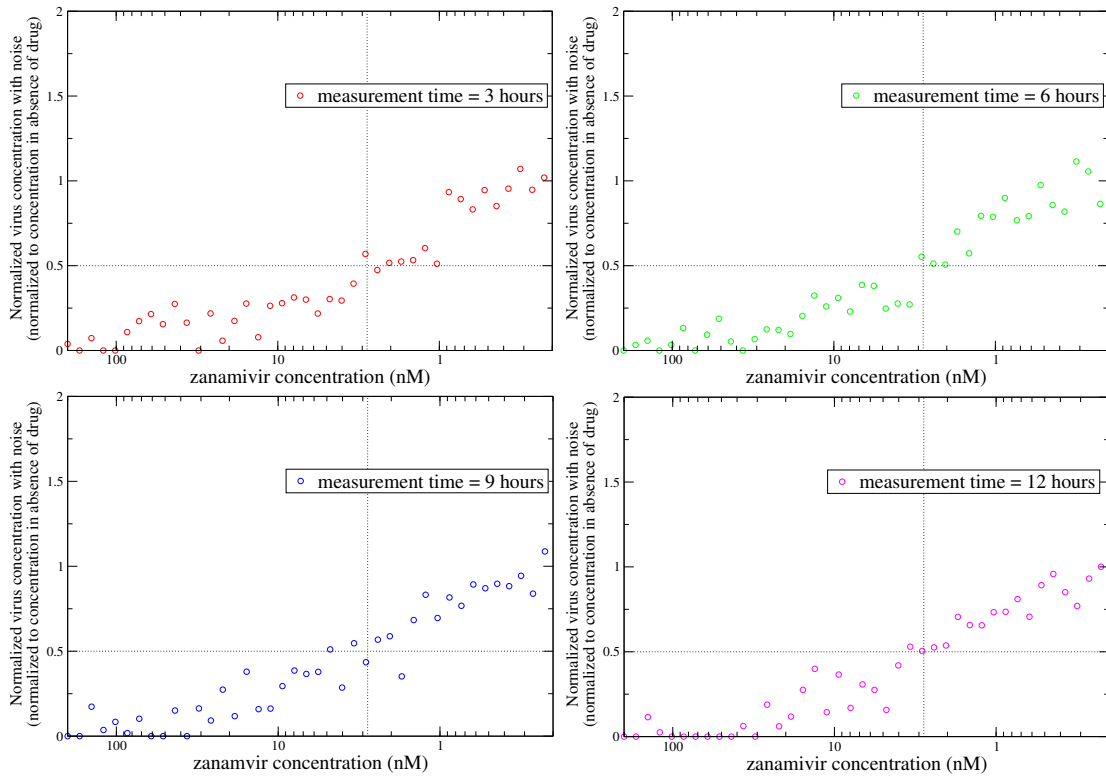


Figure 3.6: The effect of experimental variability on IC_{50} estimates from single cycle growth experiments. A Gaussian noise of 10% was added to the simulated experiments presented in Figure 3.5 to visually determine the robustness of using the single cycle growth method for estimating the IC_{50} . Here, (from left to right, and top to bottom) the virus concentrations are measured at 3, 6, 9, and 12 h. At each of the measurement times shown, the point at which both dotted lines intersect is where the input value (2.8 nM) of the IC_{50} should be.

Chapter 4

Conclusion

Antiviral drugs are very important in an influenza pandemic, since they are the main resource available for combating a pandemic at its prime. Therefore, proper characterization of the efficacy of antiviral drugs is crucial in preparing, and implementing procedures during a pandemic. The IC_{50} (the drug concentration necessary to inhibit half of a particular effect) is a widely-used technique in deciding the amount of a specific drug that would be most effective against a certain strain of virus.

There are a number of different in vitro experiments that can be performed in estimating the IC_{50} of a particular drug-strain pair. The two different methods examined in this paper include experiments that use the amount of virus as an estimate of the IC_{50} [5], and another that calculates the estimate of the IC_{50} based on cell death [13]. Although these two experimental systems utilize different components of a viral infection to extract the estimate of the IC_{50} , each systems' estimate of the IC_{50} is highly dependent upon the time at which the viral titer or the fraction of dead cells are measured. Hence, either method could lead to inconsistent

estimates of the IC_{50} because it depends on when experimentalists decide to take the measurements. Also, this could result in two incomparable estimates of the IC_{50} between two separate methods used for measuring the estimate of the IC_{50} . It is apparent through the simulations of the two separate cases for estimating the IC_{50} that these methods are very sensitive to the details of how the experiments were performed. A notable concern would be that by changing the measurement time in viral yield experiments, the estimates of the IC_{50} values can become altered by a factor of 10. And in cell viability experiments, the measurement time can influence the estimates of the IC_{50} by more than a factor of 10. Although it has not been presented in this paper, it is highly likely that this could develop into incorrect outcomes when comparing the estimates of the IC_{50} from various laboratories.

The results presented herein show that the estimate of the IC_{50} measured in the two common experiments differ from the IC_{50} values that were set as an input in the simulations using the ε_{\max} model. This is because experimentalists define the IC_{50} as the concentration of drug required to halve, for example, the population of virus or dead cells compared to that seen in the absence of drug. Thus, their estimates of the IC_{50} is defined with respect to the drug's effect on the macroscopic properties of the infection because these are the quantities that can be directly measured in experiments. On the other hand, mathematical modellers define the IC_{50} as the concentration of drug required to halve, for example, the rate at which virus is produced by an infected cell or the rate at which cells are infected by virus. Thus, their estimate of the IC_{50} is defined with respect to the drug's effect on the microscopic properties of the infection because mathematical models describe infection in terms of these microscopic properties rather than the macroscopic ones which are instead the outcome of the model.

Designing an experiment that would eliminate the variance in IC_{50} estimates due to measurement time, and that would overcome the difference between the experimental definition of the IC_{50} and the mathematical description of the IC_{50} , is fundamentally the solution to discrepancies in the estimates of IC_{50} in drug-strain pairs. We have shown that single cycle growth experiments in which all cells are infected by a large initial viral inoculum leading to a linear growth of the viral titer over time are one solution to this problem. In these experiments, the slope of the viral titer is proportional to the rate at which cells produce virus. Thus, estimating the IC_{50} from the reduction in viral titer for different drug concentrations in these experiments corresponds to extracting the effect of the drug on the microscopic infection parameter that is the viral production rate. As a result, the theoretical IC_{50} value used as an input in the simulated experiment can be recovered reliably from these experiments. In addition, we have shown that single cycle growth experiments yield estimates for the IC_{50} that are robust to changes in the variability or noise in the measurements. This makes single cycle growth experiments ideal for extracting the value of the IC_{50} for antiviral drugs which target viral production or viral release such as neuraminidase inhibitors. Unfortunately, this method cannot be used to estimate the IC_{50} of drugs which target other aspects of viral replication. In future work, we hope to explore how other experimental methods could be combined to measure the IC_{50} of any drug on each aspect of viral replication individually.

Bibliography

- [1] P. Baccam, C. Beauchemin, C. A. Macken, F. G. Hayden, and A. S. Perelson. Kinetics of influenza A virus infection in humans. *J. Virol.*, 80(15):7590–7599, August 2006.
- [2] R. D. Balicer, M. Huerta, and I. Grotto. Tackling the next influenza pandemic. *BMJ*, 328(7453):1391–1392, June 2004.
- [3] J. Carter and V. Saunders. *Virology: Principles and Applications*. Wiley, 2007.
- [4] N. J. Cooper, A. J. Sutton, K. R. Abrams, A. Wailoo, D. Turner, and K. G. Nicholson. Effectiveness of neuraminidase inhibitors in treatment and prevention of influenza a and b: systematic review and meta-analyses of randomised controlled trials. *BMJ*, 326(7401):1235, June 2003.
- [5] M. C. Eichelberger, A. Hassantoufighi, M. Wu, and M. Li. Neuraminidase activity provides a practical read-out for a high throughput influenza antiviral screening assay. *J. Virol.*, 5(1):109, 26 September 2008.
- [6] F. G. Hayden. Combination antiviral therapy for respiratory virus infections. *Antivir. Res.*, 29(1):45–48, January 1996.

- [7] J. Kreijtz, A. Osterhaus, and G. Rimmelswaan. Vaccination strategies and vaccine formulations for epidemic and pandemic influenza control. *Hum. Vaccines*, 5(3):126–135, 2009.
- [8] T. R. Maines, K. J. Szretter, L. Perrone, J. A. Belser, R. A. Bright, H. Zeng, T. M. Tumpey, and J. M. Katz. Pathogenesis of emerging avian influenza viruses in mammals and the host innate immune responses. *Immunol. Rev.*, 225(1):68–84, October 2008.
- [9] J. Maritz, L. Maree, and W. Preiser. Pandemic influenza a (h1n1) 2009: the experience of the first six months. *Clin. Chem. Lab. Med.*, 48(1):11–21, - 2010.
- [10] M. H. McCoy and E. Wang. Use of electric cell-substrate impedance sensing as a tool for quantifying cytopathic effect in influenza a virus infected mdck cells in real-time. *J. Virol.*, 130(1):157–161, December 2005.
- [11] A. S. Monto. The role of antivirals in the control of influenza. *Vaccine*, 21(16):1796–1800, May 2003.
- [12] A. Moscona. Oseltamivir resistance - disabling our influenza defenses. *New Engl. J. Med.*, 353(25):2633–2637, December 2005.
- [13] J. W. Noah, W. Severson, D. L. Noah, L. Rasmussen, E. L. White, and C. B. Jonsson. A cell-based luminescence assay is effective for high-throughput screening of potential influenza antivirals. *Antivir. Res.*, 73(1):50–59, January 2007.
- [14] M. Okomo-Adhimabo, H. T. Nguyen, K. Sleeman, T. G. Sheu, V. M. Deyde, R. J. Garten, X. Xu, M. W. Shaw, A. I. Klimov, and L. V. Gubareva. Host cell

- selection of influenza neuraminidase variants: Implications for drug resistance monitoring in a(h1n1) viruses. *Antivir. Res.*, 85(2):381–388, February 2010.
- [15] P. Palese, K. Tobita, M. Ueda, and R. W. Compans. Characterization of temperature sensitive influenza virus mutants defective in neuraminidase. *J. Virol.*, 61(2):397–410, October 1974.
- [16] J. W. Park and W. H. Jo. Computational design of novel, high-affinity neuraminidase inhibitors for h5n1 avian influenza virus. *Eur. J. Med. Chem.*, 45(2):536–541, February 2010.
- [17] G. A. Poland, R. M. Jacobson, and I. G. Ovsyannikova. influenza virus resistance to antiviral agents: a plea for rational use. *Clin. Infect. Dis.*, 48(9):1254–1256, May 2009.
- [18] A. L. Stouffer, R. Acharya, D. Salom, A. S. Levine, L. D. Costanzo, C. S. Soto, V. Tereshko, V. Nanda, S. Stayrook, and W. F. DeGrado. Structural basis for the function and inhibition of an influenza virus proton channel. *Nature*, 451(7178):596–599, January 2008.
- [19] D. M. Weinstock and G. Zuccotti. Adamantane resistance in influenza A. *JAMA*, 295(8):934–936, February 2006.

Appendix A

Solution to the single cycle growth calculations

The following is the solution for Equation 2.12, where productively-infected cell death is neglected, as was used in Section 3.3 where the single cycle growth experiment was proposed to estimate IC_{50} . Because this is a simulation for a single cycle growth experiment, all cells present at the beginning of the experiment are in the productively-infected phase of infection, I , such that

$$\begin{aligned}\frac{dI}{dt} &= -\frac{I}{\tau_I} \\ \frac{dV}{dt} &= \rho I - \frac{V}{\tau_V}\end{aligned}$$

The above equations can then be arranged into a linear non-homogeneous ordinary differential equation. From here, it is possible to solve for the virus concentration

at any given measurement time.

$$\frac{dV}{dt} + cV = \rho N$$

where V is the virus concentration, c is the clearance rate of viruses, $\rho = (1 - \varepsilon)p$, p is the viral production rate, and N is the number of productively-infected cell.

The homogeneous solution to the differential equation above is

$$\frac{dV_{\text{homo}}}{dt} + cV_{\text{homo}} = 0 \Rightarrow V_{\text{homo}} = V_{\text{homo}}(0)e^{-ct}$$

which is the general equation for solving a linear non-homogeneous ordinary differential equation. Here, the virus concentration, V , is only dependent on the initial concentration of virus, $V(0)$, viral clearance, c , and the measurement time, t . ρ is equal to zero because virus production is neglected in the homogeneous solution.

A particular solution to the differential equation leads to

$$V_p = Ae^{Bt} + C \Rightarrow \frac{dV_p}{dt} = AB e^{Bt}$$

$$\frac{dV_p}{dt} + cV_p = AB e^{Bt} + cAe^{Bt} + cC = \rho N$$

APPENDIX A. SOLUTION TO THE SINGLE CYCLE GROWTH
CALCULATIONS

where V_p is the virus concentration for a particular solution. By combining the above equation with the initial equation, the constants are solved: $A = -\frac{\rho N}{c}$, $B = -c$, and $C = \frac{\rho N}{c}$.

The full solution to the linear non homogeneous ordinary differential equation can then be written as

$$\begin{aligned} V &= V_p + V_{\text{homo}} \\ V &= Ae^{-ct} + \frac{\rho N}{c} + V_{\text{homo}}(0)e^{-ct} \end{aligned}$$

or

$$V = Ae^{-ct} + \frac{\rho N}{c}$$

At the beginning of the experiment, there are no virus present, so $V_{\text{homo}}(0)$ is equal to 0, so the entire $V_{\text{homo}}(0)e^{-ct}$ term can be removed. By rearranging the above equation, A can be substituted back into the previous equation in terms of $V(0)$, ρ , N , and c .

$$\begin{aligned} V(0) &= A' + \frac{\rho N}{c} \Rightarrow A' = V(0) - \frac{\rho N}{c} \\ V &= V_0 - \frac{\rho N}{c}e^{-ct} + \frac{\rho N}{c} \\ V(t) &= V_0e^{-ct} + \frac{\rho N}{c}(1 - e^{-ct}) \end{aligned}$$

*APPENDIX A. SOLUTION TO THE SINGLE CYCLE GROWTH
CALCULATIONS*

In the final solution, the constants A , B , and C are solved, and the virus concentration at any measurement time is characterized in terms of V_0 , c , ρ , and N . The solution effectively shows how the virus concentration from single cycle growth experiments grows linearly in time, and how it differs from multiple cycle growth experiments where virus grows exponentially in time.